Application of Adaptive Neuro-Fuzzy Inference System on Predicting Springback of U-Bending

Kun-Min Huang, Chun-Chih Kuo, Bor-Tsuen Lin*

Institute of Engineering Science and Technology, National Kaohsiung First University of Science and Technology

cck@nkfust.edu.tw

Abstract - Springback will occur when the external force is removed after bending process in sheet metal forming. This paper proposed an adaptive-network-based fuzzy inference system (ANFIS) model for prediction the springback angle of the SPCC material after U-bending. Three parameters were selected as the main factors of affecting the springback after bending, including the die clearance, the punch radius, and the die radius. The training data were obtained from results of simulated U-bending by using DYNAFORM software. The training data with four different membership functions – triangular, trapezoidal, bell, and Gaussian functions –were employed in the ANFIS to construct a predictive model for the springback of the U-bending. After the comparison of the predicted value with the checking data, we found that the triangular membership function has the best accuracy, which make it the best function to predict the springback angle of sheet metals after U-bending.

Keywords - U-bending, springback, adaptive-network-based fuzzy inference system, sheet metal forming.

I. INTRODUCTION

Bending is one of the most important processes in sheet metal forming to yield the desired shape and size. When a sheet metal is taken out of the die after the bending process, spring-back will occur, which will affect the precision and quality of products. Accordingly, minimizing the spring-back effect will avoid re-processing and greatly reduce the time and cost of die development. Livatyali and Altan[1] conducted a set of experiments and concluded that the following process parameters would heavily affect the springback in straight flanging: the punch nose radius, the die corner radius, the punch-die clearance, pad force, and the material type. In order to minimize the maximum bending load and springback. Bahloul et al. [2] proposed three optimization procedures based on the response surface method by an experimental approach. In recent years, finite element method (FEM) had been widely used to analyze the springback after bending. Cho et al. [3] investigated on springback characteristics to the major process parameters, and employed the updated Lagrangian thermo-elastoplastic finite element method to a plane-strain sheet metal U-bending process. They found that the punch corner radius, the punch-die clearance and the friction coefficient had the most impact on the springback.

The results of springback simulated by FEM may vary according to how numerical parameters are set. Sousa et al. [4] coupled the forming analysis software with the evolutionary genetic algorithm searching the optimal design parameters of the V- and U-bending processes. Levy [5] constructed an experimental equation to predict the degree of springback, and took the yield strength, bending radius, die clearance, and the thickness of the sheet metal into consideration. The adaptive network fuzzy inference system (ANFIS) was first introduced by Jang in 1993 [6]. Lin and Liu [7] adopted an ANFIS to predict the surface roughness of the chemical-mechanical polishing processes. Sharma et al. [8] estimated the tool wear rate in turning operations using ANFIS. Hayati et al. [9] developed ANFIS model for prediction of the heat transfer rate of the wire-on-tube type heat exchanger. Yeh et al. [10] combined ANFIS, FEM and true strain method to determine the anisotropic optimum blank in stretch flange process.

This paper presents the implementation of the ANFIS to predict the springback angle of the SPCC sheet metal after U-bending. Three parameters were selected as the main factors of affecting the spring-back (SB) after bending, including the die clearance (DC), the punch radius (PR), and the die radius (DR), were simulated by the sheet metal forming analysis software DYNAFORM V5.1. We obtain the training data of the ANFIS from FEM result. In predicted model of ANFIS, four different types of membership functions (triangular function, trapezoidal function, bell function, and Gaussian function) were adopted. The results from the four developed prediction models were compared with the verification data to confirm the feasibility of this approach.

II. ANFIS APPROACH

ANFIS is employed to model the relationship between the features of bending parameters and vibration signal with the measured values of springback. The architecture of ANFIS was first introduced by Jang in 1993[11]. To apply the ANFIS, we consider three inputs DC, PR, and DR, and a single output SB in the fuzzy inference system. The architecture of ANFIS used in this paper is shown in Figure 1. The Sugeno fuzzy model is utilized in fuzzification and defuzzification of the system. For a first-order Sugeno fuzzy model, a typical rule set with 27 fuzzy if-then rules can be expressed as:

Rule *n*: If (DC is A_i) and (PR is B_j) and (DR is C_k) then

$$(f_{ijk} = p_{ijk}DC + q_{ijk}PR + r_{ijk}DR + s_{ijk})$$

where $n = i + (j-1)\times 3 + (k-1)\times 9$ (i, j, k = 1, 2, 3) , A_i, B_j and C_k (i, j, k = 1, 2, 3) are the linguistic terms of the precondition part with membership functions $\mu_{A_i}(DC)$,

$\mu_{B_j}(PR)$ and $\mu_{C_k}(DR)$, p_{ijk}, q_{ijk}, r_{ijk} and s_{ijk} $(i, j, k = 1, 2, 3)$ are the consequent parameters, and f_{ijk} is the output variable.

The complete ANFIS consists of five layers, the fuzzy layer, production layer, normalization layer, de-fuzzy layer, and total output layer. Each layer involves several nodes, which are described by the node function. The node function in each layer, which performs the same operation, is detailed below:

Layer 1 is the fuzzy layer, in which every node is an adaptive node with node function as:

$$O_{A_i}^1 = \mu_{A_i}(DC),\ i = 1, 2, 3.$$
$$O_{B_j}^1 = \mu_{B_j}(PR),\ j = 1, 2, 3.$$
$$O_{C_k}^1 = \mu_{C_k}(DR),\ k = 1, 2, 3.$$

where *DC*, *PR* and *DR* are the inputs of nodes, μ_{A_i}, μ_{B_j} and μ_{C_k} denote the membership functions of the fuzzy set. Four different types of membership functions (triangular function, trapezoidal function, bell function, and Gaussian function) were adopted in this paper. The equations of each of the aforementioned membership functions are detailed below:

1. Triangular membership function:

$$\mu_{A_i}(x, a_{A_i}, b_{A_i}, c_{A_i}) = \begin{cases} 0 & for\ x < a_{A_i} \\ \dfrac{(x - a_{A_i})}{(b_{A_i} - a_{A_i})} & for\ a_{A_i} \le x \le b_{A_i} \\ \dfrac{(c_{A_i} - x)}{(c_{A_i} - b_{A_i})} & for\ b_{A_i} \le x \le c_{A_i} \\ 0 & for\ x > c_{A_i} \end{cases}$$

where a_{A_i}, b_{A_i}, and c_{A_i} are parameters, and x is a variable.

2. Trapezoidal membership function:

$$\mu_{A_i}(x, a_{A_i}, b_{A_i}, c_{A_i}, d_{A_i}) = \begin{cases} 0 & for\ x < a_{A_i} \\ \dfrac{(x - a_{A_i})}{(b_{A_i} - a_{A_i})} & for\ a_{A_i} \le x \le b_{A_i} \\ 1 & for\ b_{A_i} \le x \le c_{A_i} \\ \dfrac{(d_{A_i} - x)}{(d_{A_i} - c_{A_i})} & for\ c_{A_i} \le x \le d_{A_i} \\ 0 & for\ x > d_{A_i} \end{cases}$$

where a_{A_i}, b_{A_i}, c_{A_i}, and d_{A_i} are parameters, and x is a variable.

3. Bell membership function:

$$\mu_{A_i}(x, a_{A_i}, b_{A_i}, c_{A_i}) = \frac{1}{1 + \left| \dfrac{x - c_{A_i}}{a_{A_i}} \right|^{2b_{A_i}}}$$

where a_{A_i}, b_{A_i}, and c_{A_i} are parameters, and x is a variable.

4. Gaussian membership function:

$$\mu_{A_i}(x, c_{A_i}, \sigma_{A_i}) = e^{-\frac{(x - c_{A_i})^2}{\sigma_{A_i}^2}}$$

where c_{A_i} and σ_{A_i} are parameters, and x is a variable.

In each membership function, the parameters can be treated as premise parameters.

Layer2 is the production layer, in which every node is a fixed node with node function to multiply input signals to serve as output signal:

$$O_{ijk}^2 = \mu_{A_i}(DC) \times \mu_{B_j}(PR) \times \mu_{C_k}(DR) = w_{ijk},$$
$$i, j, k = 1, 2, 3.$$

where w_{ijk} represents the firing strength of a rule.

Layer3 is the normalization layer, in which every node is a fixed node with node function to normalize firing strength by calculating the ratio of this node firing strength to the sum of the firing strength:

$$O_{ijk}^3 = \bar{w}_{ijk} = \frac{w_{ijk}}{\sum_i \sum_j \sum_k (w_{ijk})},\ i, j, k = 1, 2, 3.$$

where $\bar{w}_{ijk}$ denotes the normalized firing strength.

Layer 4 is the de-fuzzy layer, in which every node is an adaptive node with node function to compute the consequence of each fuzzy rule using the following formula:

$$O_{ijk}^4 = \bar{w}_{ijk} f_{ijk} = \bar{w}_{ijk}(p_{ijk}(DC) + q_{ijk}(PR) + r_{ijk}(DC) + s_{ijk}),$$
$$i, j, k = 1, 2, 3.$$

Layer 5 is the total output layer, in which the single node is a fixed node with node function to calculate the overall output:

$$SB = O_1^5 = \sum_{i=1}^{3} \sum_{j=1}^{3} \sum_{k=1}^{3} \bar{w}_{ijk} f_{ijk},\ i, j, k = 1, 2, 3.$$

where SB denotes the inferred output (i.e., the predicted springback angle) of the ANFIS.

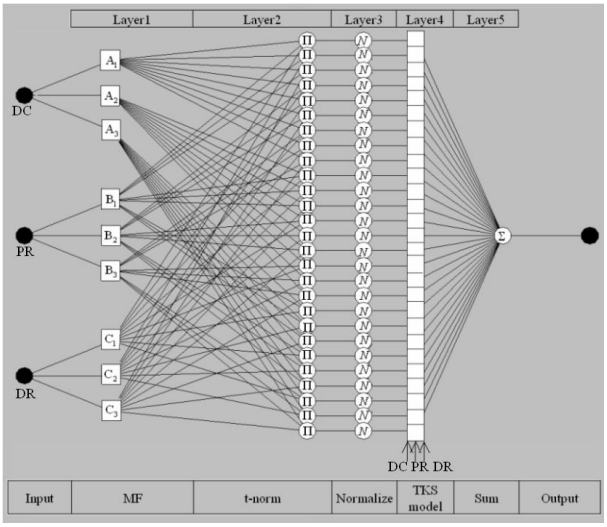

Fig. 1. The frameworks of ANFIS

III. EXPERIMENTS and COMPUTATIONS

A. Experimental Factors Planning

In this paper, we discuss the factors that affect the SB after U-bending. These factors include the DC, PR, and DR, as shown in Figure 2. First, we set four levels for each of the factors of the prediction model. For the DC, we decide the mean value of four chosen values that equals thickness of sheet metal as the basis. Then, we choose two values that are smaller than the basis and two values that is greater than the basis, with an incremental value of 1/10 of the basis. The four levels for the DC are 0.425mm, 0.475mm, 0.525mm, and 0.575mm. For the PR, we choose PR =1mm as the basis with an incremental value of 2mm. The four levels for the PR are 1mm, 3mm, 5mm, and 7mm. For the DR, we choose DR =2mm as the basis with an incremental value of 2mm. The four levels for the DR are 2mm, 4mm, 6mm, and 8mm. Therefore, there are 64 different combinations, as shown in Table 1. The simulation result of each combination is used to construct the model to predict the SB angle.

In addition, we set the levels for each of the factors of the checking model, where the value of each level is the mean value of the corresponding values in the prediction model. Therefore, the two levels of the DC are 0.5mm and 0.55mm. The three levels of the PR are 2mm, 4mm, and 6mm. The three levels of the RD are 3mm, 5mm, and 7mm. There are a total of 18 different combinations, as shown in Table 2. The verification data of each combination are used to verify the accuracy of the prediction model.

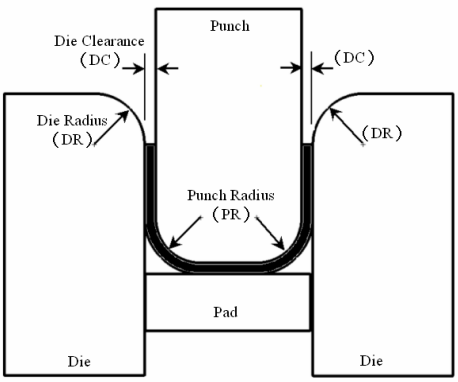

Fig. 2. Definition of die parameters.

B. Finite Element Model

We use the commercial software DYNAFORM V5.1 and calculator LS-DYNA to perform bending and SB simulation. Figure 3 shows the simulation process. First, the different combinations of factors detailed in Table 1 is used to construct the U-shaped bending model, which includes the punch, the die, the pad, and the blank, as shown in Figure 4(a). Then, the model is meshed by the shell element, as shown in Figure 4(b).

In this simulation, we use the SPCC as the material. The size of the sheet is 70mm × 30mm × 0.5mm. A summary of the characteristics of the sheet is shown in Table 3. The material type in LS-DYNA is type 37. The coefficient of friction between dies and the sheet is set to 0.25.

Figure 5 shows the several states during the bending process. First, a pressing force is applied to the pad, which brings it into contact with the blank. Then, the punch starts to move downward with a speed of 100mm/s, and stops moving as soon as it reaches the desired depth. Next, the punch starts to move upwards with a speed of 100mm/s to finish the bending process. Finally, the blank is spring back when the external forces and constraints are removed. Table 1 shows the simulation results of the SB.

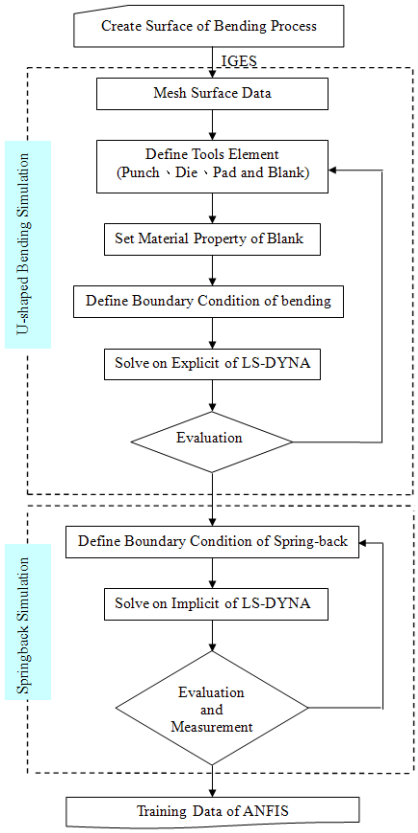

Fig. 3. The flowchart of bending and spring-back simulation.

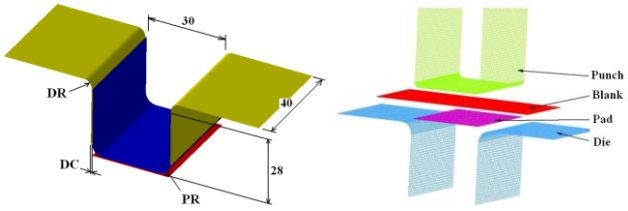

(a) (b)

Fig. 4. Simulated model. (a) dimension definition; (b) finite element mesh.

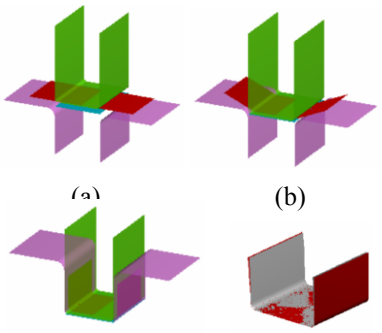

(a) (b)

(c) (d)

Fig. 5. Simulation process of bending and springback. (a) holding. (b) bending. (c) final bending (d) springback.

Table 1. Comparison between the simulated and predicted springback under different membership functions

NO.	Parameters			Simulated *SB*(degree)	Predicted *SB* (degree)			
	DC (mm)	*PR* (mm)	*DR* (mm)		Triangular membership function	Trapezoidal membership function	Bell membership function	Gaussian membership function
T1	0.425	1	2	0.87	0.87	0.87	0.88	0.87
T2	0.425	1	4	0.92	0.92	0.92	0.91	0.91
T3	0.425	1	6	1.02	1.02	1.02	1.03	1.03
T4	0.425	1	8	1.16	1.16	1.16	1.15	1.16
T5	0.425	3	2	1.44	1.43	1.44	1.43	1.43
T6	0.425	3	4	1.58	1.59	1.58	1.58	1.57
T7	0.425	3	6	1.92	1.93	1.91	1.94	1.93
T8	0.425	3	8	2.28	2.27	2.29	2.28	2.28
T9	0.425	5	2	1.91	1.91	1.91	1.92	1.92
T10	0.425	5	4	2.03	2.03	2.03	2.03	2.05
T11	0.425	5	6	2.47	2.46	2.48	2.45	2.45
T12	0.425	5	8	2.89	2.90	2.88	2.89	2.89
T13	0.425	7	2	2.36	2.36	2.36	2.36	2.36
T14	0.425	7	4	2.44	2.43	2.44	2.43	2.43
T15	0.425	7	6	2.82	2.83	2.82	2.84	2.83
T16	0.425	7	8	3.30	3.29	3.30	3.29	3.30
T17	0.475	1	2	0.95	0.94	0.95	0.95	0.95
T18	0.475	1	4	1.09	1.10	1.09	1.09	1.09
T19	0.475	1	6	1.30	1.29	1.30	1.29	1.30
T20	0.475	1	8	1.48	1.48	1.48	1.48	1.48
T21	0.475	3	2	1.78	1.79	1.78	1.79	1.79
T22	0.475	3	4	2.05	2.02	2.05	2.03	2.03
T23	0.475	3	6	2.31	2.32	2.33	2.34	2.33
T24	0.475	3	8	2.53	2.53	2.52	2.52	2.52
T25	0.475	5	2	2.69	2.68	2.69	2.69	2.68
T26	0.475	5	4	2.96	2.98	2.96	2.98	2.99
T27	0.475	5	6	3.40	3.39	3.38	3.38	3.37
T28	0.475	5	8	3.60	3.60	3.61	3.61	3.61
T29	0.475	7	2	3.31	3.31	3.31	3.31	3.31
T30	0.475	7	4	3.73	3.73	3.73	3.73	3.72
T31	0.475	7	6	4.28	4.27	4.28	4.28	4.29
T32	0.475	7	8	4.57	4.57	4.57	4.57	4.57
T33	0.525	1	2	1.35	1.35	1.35	1.34	1.34
T34	0.525	1	4	1.49	1.50	1.50	1.51	1.52
T35	0.525	1	6	1.73	1.72	1.68	1.71	1.70
T36	0.525	1	8	1.86	1.86	1.90	1.87	1.87
T37	0.525	3	2	3.12	3.13	3.15	3.14	3.16
T38	0.525	3	4	3.41	3.39	3.40	3.38	3.39
T39	0.525	3	6	3.57	3.59	3.57	3.59	3.58
T40	0.525	3	8	3.75	3.74	3.71	3.73	3.71
T41	0.525	5	2	4.06	4.05	4.04	4.04	4.01
T42	0.525	5	4	4.23	4.25	4.23	4.25	4.25
T43	0.525	5	6	4.48	4.46	4.49	4.47	4.48
T44	0.525	5	8	4.61	4.62	4.64	4.62	4.65
T45	0.525	7	2	4.93	4.93	4.93	4.93	4.94
T46	0.525	7	4	5.28	5.27	5.28	5.29	5.29
T47	0.525	7	6	5.62	5.63	5.63	5.60	5.60
T48	0.525	7	8	5.80	5.80	5.80	5.81	5.80
T49	0.575	1	2	2.03	2.03	2.03	2.03	2.04
T50	0.575	1	4	2.27	2.28	2.26	2.27	2.25
T51	0.575	1	6	2.47	2.46	2.52	2.46	2.49
T52	0.575	1	8	2.78	2.78	2.74	2.78	2.77
T53	0.575	3	2	3.77	3.78	3.74	3.78	3.75
T54	0.575	3	4	3.97	3.95	3.97	3.95	3.95
T55	0.575	3	6	4.06	4.08	4.09	4.09	4.10
T56	0.575	3	8	4.20	4.19	4.22	4.19	4.21
T57	0.575	5	2	4.61	4.60	4.63	4.61	4.63
T58	0.575	5	4	4.80	4.82	4.80	4.82	4.84
T59	0.575	5	6	5.06	5.04	5.01	5.04	5.01
T60	0.575	5	8	5.16	5.17	5.15	5.17	5.15
T61	0.575	7	2	5.38	5.38	5.38	5.38	5.38
T62	0.575	7	4	5.76	5.75	5.76	5.76	5.74
T63	0.575	7	6	5.98	5.99	5.97	5.98	6.00
T64	0.575	7	8	6.11	6.11	6.11	6.11	6.11
					1.18	1.66	1.30	1.92

Table 2. Comparison between the simulated and predicted springback under different membership functions

NO.	Parameters			Simulated *SB*(degree)	Predicted *SB* (degree)			
	DC (mm)	*PR* (mm)	*DR* (mm)		Triangular membership function	Trapezoidal membership function	Bell membership function	Gaussian membership function
C1	0.50	2	3	2.01	2.07	0.70	0.57	1.72
C2	0.50	2	5	1.95	2.37	1.02	1.36	1.71
C3	0.50	2	7	2.19	2.51	1.20	2.03	1.88
C4	0.50	4	3	2.95	3.24	2.23	2.26	2.91
C5	0.50	4	5	3.25	3.66	2.67	3.77	2.97
C6	0.50	4	7	3.49	3.71	3.26	4.14	3.24
C7	0.50	6	3	4.31	4.12	3.42	4.03	3.56
C8	0.50	6	5	4.4	4.57	4.00	4.90	3.86
C9	0.50	6	7	4.51	4.75	4.30	5.38	4.17
C10	0.55	2	3	2.52	2.57	0.55	0.95	2.45
C11	0.55	2	5	2.65	2.79	0.73	1.81	2.74
C12	0.55	2	7	2.79	2.96	0.94	2.47	2.97
C13	0.55	4	3	3.79	3.97	2.35	3.29	4.61
C14	0.55	4	5	4.03	4.23	3.21	4.81	4.38
C15	0.55	4	7	4.1	4.38	4.64	4.99	4.47
C16	0.55	6	3	4.69	4.70	5.00	5.26	4.92
C17	0.55	6	5	5.12	5.01	5.45	6.23	5.16
C18	0.55	6	7	5.35	5.20	5.61	6.52	5.25
				RMSE(%)	22.88	104.79	83.50	36.45

Table3. Material properties of SPCC

Parameter	**Value**
Sheet thickness	0.5**mm**
Mass density	7.83×10^{-9}**Ton / mm**^{3}
Young's Modulus	207**GPa**
Poisson's ratio	0.3
Yield stress	150**MPa**
Tensile strength	315**MPa**
Anisotropic factor	1.7
Strain hardening exponent	0.21
Strength coefficient	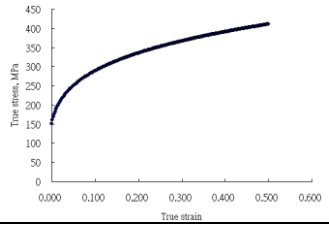

C. Construction of the ANFIS System

We used the ANFIS theory to construct the model to predict the SB angle after bending. MATLAB 7.01 Fuzzy Logic Toolbox was used in our research. The simulated results of the SB angle for U-shape bending are used as the training data (64 groups, as shown in Table 1) for the prediction model. The training data has three input parameters (the DC, PR and DR), and one output (the SB angle), as shown in Figure 6. First we load the training data into MATLAB Fuzzy Logic Toolbox, and choose a membership function. We can choose different membership functions for each of the input parameters. The chosen membership functions are triangular membership function, trapezoidal membership function, bell membership function, and Gaussian membertship function. After the model is trained using the hybrid- learning rule, the results output by different membership functions were verified against the verification data (18 groups, as shown in Table 2). The accuracy of each membership function is determined using the root-mean-square-error (RMSE). The prediction model with the smallest RMSE is the best.

System ANAFIS: 3 input, 1 output, 27 rules

Fig. 6. Fuzzy rule architecture of ANFIS model.

IV. RESULTS AND DISCUSSIONS

A. Comparison of Prediction Models Using Different Membership Functions

Table 1 shows the RMSE for each of the result output by the aforementioned four different membership functions. Comparing with the training values, the RMSE of the predicted springback degrees output by triangular

membership function, trapezoidal membership function, bell membership function, and Gaussian membership function are 1.18%, 1.66%, 1.30%, and 1.92% respectively. The prediction model using triangular membership function has the smallest RMSE.

Figure 7-9 shows the comparison between the triangular membership function of the three input parameters before and after the training respectively. As shown in the figures, the triangular membership function of the DC and PR differs greatly before and after the training, and the triangular membership functions of the DR changed locally before and after the training.

Moreover, the 18 groups of verification data were fed into the prediction models those were constructed using the triangular, trapezoidal, bell and Gaussian membership functions. The ERMS of the output are 22.88%, 104.79%, 83.50%, and 36.45% respectively, as shown in Table 2. Therefore, the prediction model using triangular membership function also has the smallest RMSE and the best predictive value.

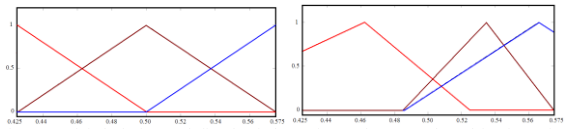

Fig. 7. Initial (left) and final (right) triangular membership function of die clearance (DC).

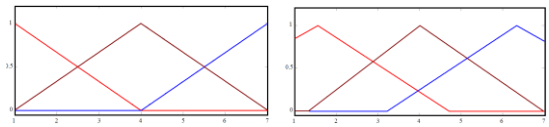

Fig. 8. Initial (left) and final (right) triangular membership function of punch radius (PR).

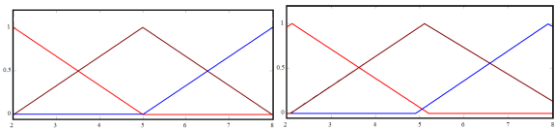

Fig.9. Initial (left) and final (right) triangular membership function of die radius (DR).

B. Impact of the Bending Parameters on the SB

Figure 10-12 show the impacts of the DC, PR, and DR on the SB for U-shape bending. The smaller the DC, the smaller the SB angle, because the smaller clearance generated higher compressive stress in the bending area of the sheet during the bending process can reduce larger force that brings the sheet back to its original shape. A smaller PR can also reduce the SB angle, since sheets are subject to greater bending. The purpose of the DR is to make the bending process easier. As shown in the figure, it has a very small impact on the SB. Therefore, the SB angle is proportional to the DC, and the PR, and the DR.

From Figure 10, it can be seen that the slopes of PR is higher than the slopes of DR. In Figure 12, the slopes of PR is higher than that of DC. Therefore, PR has the most impact on the SB.

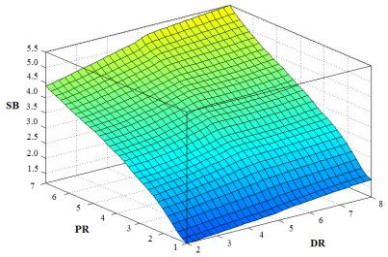

Fig.10. Contour surface for the DR and PR on the SB

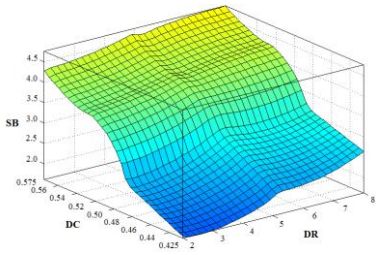

Fig.11. Contour surface for the DR and DC on the SB

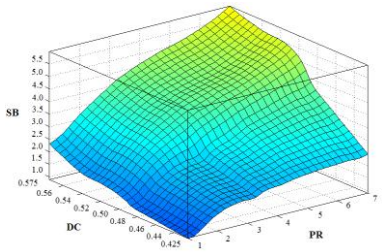

Fig.12. Contour surface for the PR and DC on the SB

V. CONCLUSIONS

Our research used the ANFIS and the training data collected by the finite element method to construct the predicted model to forecast the springback angle for U-shape bending. The predicted model was verified by comparing the predicted values with the checking data. Based on our research, we have drawn the following conclusions:

The model constructed using the ANFIS theory can effectively predict the springback angle of U-shape bending by using three bending parameters (die clearance, the punch radius, and the die radius).

We used the ANFIS to train four different membership functions to determine the most suitable model. The prediction model using triangular membership function has the smallest RMSE (0.0118) after the training. The 18 groups of verification data were fed into the prediction model that was constructed using the triangular membership function. The RMSE of the output is 0.2288, which is also the smallest. We can obtain that the most suitable membership function is the triangular membership function.

REFERENCES

[1] Livatyali H, Altan T (2001) Prediction and elimination of springback in straight flanging using computer aided design methods Part 1. Experimental investigations. J. Mater. Process. Technol. 117 262-268.

[2] Bahloul R, Ayed LB, Potiron A, Batoz JL (2009) Comparison between three optimization methods for the minimization of maximum bending load and springback in wiping die bending obtained by an

experimental approach. Int. J. Adv. Manuf. Technol. DOI 10.1007/s00170-009-2332-0 (online)

[3] Cho JR, Moon SJ, Moon YH, Kang SS (2003) Finite element investigation on spring-back characteristics in sheet metal U-bending process. J. Mater. Process. Technol. 141 109-116.

[4] Sousa LC, Castro CF, Antonio CAC (2006) Optimal design of V and U bending processes using genetic algorithms. J. Mater. Process. Technol. 172 35-41.

[5] Levy BS (1984) Empirically derived equations for predicting springback in bending. J. Appl. Metalworking 3 135-141.

[6] Jang JSR (1993) ANFIS : Adaptive-network-based fuzzy inference systems. IEEE Trans. Syst. Man Cybern. 23 3 665-685.

[7] Lin ZC, Liu CY (2001) Application of an Adaptive Neuro-Fuzzy Inference System for the Optimal Analysis of Chemical-Mechanical Polishing Process Parameter. Int. J. Adv. Manuf. Technol. 18 20-28.

[8] Sharma VS, Sharma SK, Sharma AK (2008) Cutting tool wear estimation for turning. Int. J. Adv. Manuf. Technol. 19 99-108.

[9] Hayati M, Rezaei A, Seifi M (2009) Prediction of the heat transfer rate of a single layer wire-on-tube type heat exchanger using ANFIS. Int. J. Refrig. 32 1914-1917.

[10] Yeh FH, Wu MT, Li CL (2007) Accurate optimization of blank design in stretch flange based on a forward-inverse prediction scheme. Int. J. Mach. Tools Manuf. 47 1854-1863.